Observer of the human cardiac sympathetic nerve activity using non-causal blind source separation

R. Vetter[1], **P. Celka**[1], **J.-M. Vesin**[1] **and U. Scherrer**[2]

[1]Signal Processing Laboratory, Swiss Federal Institute of Technology, 1015 Lausanne, Switzerland

[2]Department of Internal Medicine, University Hospital, 1011 Lausanne, Switzerland

RÉSUMÉ

Nous présentons une méthode pour la reconstruction aveugle de deux variables de contrôle du système cardiovasculaire en utilisant seulement le rythme cardiaque et la tension artérielle. Le modèle de reconstruction est basé sur la séparation aveugle de source dans des mélanges convolutifs. L'algorithme d'apprentissage associé est déduit d'une approche de maximisation d'information.

L'efficacité de la méthode a été verifiée en utilisant l'activité musculaire sympathique comme indicateur de l'activité cardiaque sympathique. Des résultats très satisfaisants et prometteurs ont été obtenus sur les signaux de cinq sujets.

ABSTRACT

We present a method for the blind reconstruction of two control variables of the cardiovascular system using only heart rate and arterial blood pressure. The reconstruction system is based on a model for blind source separation of convolutive mixtures. The associated learning scheme is deduced from an information maximization approach. The efficiency of the method has been verified using the muscle sympathetic nerve activity as an indicator for the cardiac sympathetic nerve activity. Very satisfying and promising results have been obtained for five subjects.

1 Introduction

It is well established that heart rate (HR) and arterial blood pressure (ABP) fluctuations are generated by a complex regulation system. Spontaneous fluctuations in heart rate have been separated into three spectral bands: very low frequency oscillations (VLF range: 0.008-0.04Hz) attributable to thermal regulations, low frequency fluctuations (LF range: 0.04-0.15Hz) due to arterial baroreceptor modulation, and high-frequency components (HF range: 0.15-0.4Hz) that include the respiratory sinus arrhythmia [1]. We focus in this paper on the LF oscillations mediated to the baroreceptor control loop represented by figure 1. We can point out that the central control variables of the baroreceptor loop are the two antagonistic parts of the autonomic nervous system: the cardiac sympathetic ($CSNA$) and parasympathetic ($CPNA$) nervous activities. Both $CSNA$ and $CPNA$ play a key role in cardiovascular regulation. For several reasons, information about the dynamics of $CSNA$ and $CPNA$ could be useful for analysis and diagnosis in clinical applications. It has been reported for example that several diseases (e.g diabetes) may cause a dysfunction of the autonomic nervous system. There is also experimental evidence that high sympathetic activity during myocardial infarction greatly increases the probability of a fatal cardiac arrhythmia [2]. However, $CSNA$ and $CPNA$ are inaccessible signals in humans and it would be desirable to have a model allowing the reconstruction of these hidden variables.

We present a method for building an observer of $CSNA$ and $CPNA$ in the LF band using blind source separation (BSS) techniques . Such techniques can be applied successfully if we assume that the baroreceptor loop of figure 1 can be modeled by a linear system [1]. Thus, HR and ABP are
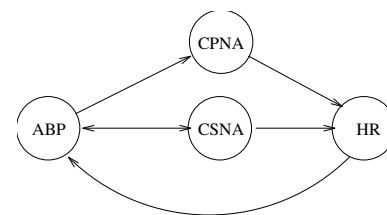

Figure 1 — Baroreflex control loop

non-causal linear mixtures of $CSNA$ and $CPNA$. The problem consists therefore of reconstructing hidden source signals ($CSNA$, $CPNA$) using only linear mixtures of these signals (HR, ABP) which is the classical problem of BSS. It can be solved if the hidden signals ($CSNA$, $CPNA$) are statistically independent. Although mutual independence of $CSNA$ and $CPNA$ has not been reported yet, whereas it has been shown in [3] that reciprocal relationships exist between the sympathetic and the parasympathetic outflows in the baroreceptor reflex. Therefore, *mutual independence* of these signals will be our basic assumption and non-causal BSS can be applied to blind reconstruction of $CSNA$ and $CPNA$. In this paper we present a BSS based on the information maximization approach introduced by Bell and Sejnowski [4]. The proposed method as well as numerical simulations on synthetic signals are presented in section 3. In section 4, the developed observer is applied to the cardiovascular system.

2 Data acquisition

General procedure: subjects are all a subset of different previous studies. They have been chosen in order to be representa-

tive of high muscle sympathetic nerve activity ($MSNA$). After providing informed consent, we obtained from 5 quietly resting subjects simultaneous measurements of heart rate, arterial blood pressure (Finapres Ohmeda, Englewood) and efferent $MSNA$ [5]. Signals have been recorded continuously on an electrostatic recorder and sampled at 500 Hz on a 486 intel PC with an A/D board (Labmaster).

MSNA procedure: multi-unit fibre recordings of efferent $MSNA$ have been obtained with unipolar tungsten microelectrodes inserted selectively into muscle nerve fascicles of the peroneal nerve posterior to the fibular head by the microneurographic technique of Vallbo *et al.* [5]. The neural signals have been amplified (by 20-50 $\times 10^3$), filtered (700-2000 Hz), rectified and integrated (time constant 0.1 s).

Data analysis: all signals (ABP, ECG and $MSNA$) have been acquired during 360 s. The $MSNA$ signal has been processed with linear and nonlinear morphological filters in order to suppress all artifacts and noise. The resulting nerve signal was then post-processed using an adaptive sliding integration depending on the preceding HR value throughout the data. Finally, all signals have been re-sampled at 1.4 Hz and sets $\{ABP, HR, MSNA\}$ with jointly stationary signals have been selected.

3 Blind source separation

BSS has been introduced by Jutten and Herault in [6] and has received since then increasing attention from the signal processing community. We consider in this paper a model for non-causal linear BSS. The observed signals (x_1, x_2) are given by

$$x_1(n) = s_1(n) + \sum_{i=-p_{12nc}}^{p_{12c}-1} h_{12}(i)s_2(n-i) \qquad (1)$$

$$x_2(n) = s_2(n) + \sum_{i=-p_{21nc}}^{p_{21c}-1} h_{21}(i)s_1(n-i) \qquad (2)$$

where s_1,s_2 are the hidden source signals, $\{h_{ij}\}$ the non-causal linear coupling filters and $p_{ij} = p_{ijnc} + p_{ijc}$ their order for $i, j = 1, 2$ and $i \neq j$.

Throughout this paper the following assumptions hold for the source signals (s_1,s_2): they are statistically independent, not jointly Gaussian and of unit variance. Furthermore, we assume that we have some knowledge about the shape of their probability density functions (pdf).

The aim of BSS is the reconstruction of the hidden source signals ($s1$, $s2$) using only an observed mixture (x_1, x_2) of these signals. In order to reach this goal we choose a feedback model instead of a feed forward implementation because it does not need post-processing. Thus, the reconstructed signals (u_1, u_2) are given by

$$u_1(n) = x_1(n) - \sum_{i=-p_{12nc}}^{p_{12c}-1} w_{12}(i)u_2(n-i) \qquad (3)$$

$$u_2(n) = x_2(n) - \sum_{i=-p_{21nc}}^{p_{21c}-1} w_{21}(i)u_1(n-i) \qquad (4)$$

where $\{w_{12}\}$ and $\{w_{21}\}$ are the de-mixing filters.

The reconstruction system contains a feedback part and therefore stability requirements have to be fulfilled. By applying the Nyquist criterion we obtain

$$K = \sum_{k=-\infty}^{\infty} |w(k)| < 1 \qquad (5)$$

where $w(k) = \sum_{l=-\infty}^{k} w_{12}(l)w_{21}(k-l)$. Hence $K < 1$ is a sufficient condition for the stability of the global system.

3.1 Learning algorithm

The learning of the de-mixing parameters requires the use of higher order statistics (HOS) [6]. Two main classes of methods can be distinguished: those that implicitly take some aspects of HOS into account through nonlinear functions of the reconstructed signals, and those that do it explicitly (for historical references see [4, 7]). For the first class, Bell and Sejnowski have presented the basis for a more theoretical framework. They proposed to deduce an update rule for the de-mixing parameters from the differential entropy of nonlinear functions g_i of the reconstructed signals: $y_i = g_i(u_i), i = 1, 2$. It can be shown that maximization of this criterion corresponds to the minimization of the mutual information between the components (y_1, y_2) if (g_1, g_2) are chosen in order to optimally match the pdfs of the source signals.

Applications of this approach to feedback systems have been presented in [7, 8] and will constitute the basis of our work. The entropy of the output is given by $H(\mathbf{y}) = -\mathrm{E}[\ln(f_\mathbf{y}(\mathbf{y}))]$, where $f_\mathbf{y}(\mathbf{y})$ is the pdf of $\mathbf{y}$ and $\mathbf{y} = [y1 \ y2]^T$. Using the relation $f_\mathbf{y}(\mathbf{y}) = f_\mathbf{x}(\mathbf{x})/|J|$, where $|J|$ is the absolute value of the Jacobian of the reconstruction network and $\mathbf{x} = [x1 \ x2]^T$, we obtain

$$H(\mathbf{y}) = \mathrm{E}[\ln(|\mathrm{J}|)] - \mathrm{E}[(\ln(f_\mathbf{x})] \qquad (6)$$

The second term represents the entropy of $\mathbf{x}$ and remains unaffected by alterations of the de-mixing parameters. Therefore, maximizing the entropy of the outputs reduces to maximizing the Jacobian of the network. The application of a stochastic gradient algorithm to equation (6) leads to the following update rule for w_{12}

$$\Delta w_{12}(k) \propto \frac{\partial}{\partial w_{12}(k)}(ln|J|) \qquad k = p_{12nc}\ldots p_{12c} - 1 \quad (7)$$

This function can be developed as

$$\Delta w_{12}(k) \propto \frac{1}{g_1'}\frac{\partial g_1'}{\partial w_{12}} + \frac{1}{g_2'}\frac{\partial g_2'}{\partial w_{12}} + \frac{1}{D}\frac{\partial D}{\partial w_{12}} \qquad (8)$$

where $g_1' = \frac{\partial g_1}{\partial u_1}$, $g_2' = \frac{\partial g_2}{\partial u_2}$ and $D = \frac{\partial u_1}{\partial x_1}\frac{\partial u_2}{\partial x_2} - \frac{\partial u_1}{\partial x_2}\frac{\partial u_2}{\partial x_1}$. It can be shown that the term $\frac{1}{D}\frac{\partial D}{\partial w_{12}}$ do not depend on reconstructed signals. Therefore we neglect it and obtain

$$\Delta w_{12}(k) \propto [f_1(u_1) \ f_2(u_2)]\frac{\partial \mathbf{u}}{\partial w_{12}(k)} \qquad (9)$$

where $\mathbf{u} = [u1 \ u2]^T$ and $f_i(u_i) = \frac{1}{g_i'}\frac{\partial^2 g_i}{\partial u_i^2}$. In order to determine the derivative of (3) and (4) we transform these equations into

$$\mathbf{u}(n) = (\mathbf{I} + \mathbf{W}_0)^{-1}\{\mathbf{x}(n) - \sum_{k=-\infty, k\neq 0}^{\infty} \mathbf{W}_k\mathbf{u}(n-k)\} \qquad (10)$$
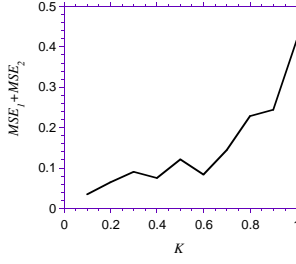
Figure 2 — Results for various coupling factors

where $\mathbf{x} = [x1 \; x2]^T$, $\mathbf{s} = [s1 \; s2]^T$, the matrices $\mathbf{W}_k$ contain the elements $w_{ij}(k)$ for $i, j = 1, 2$ and $i \neq j$, and $\mathbf{I}$ is the identity matrix. Finally we can determine the update rule using equations (9) and (10) and we obtain (similar for $\mathbf{w}_{21}$)

$$\mathbf{w}_{12}(n+1) = \mathbf{w}_{12}(n) + \mu\alpha\{f_1(u_1(n))\mathbf{u}_2(n)\} \qquad (11)$$

where $\mathbf{w}_{12} = [w_{12}(p_{12nc})...w_{12}(p_{12c}-1)]^T$, $\mathbf{u}_2(n) = [u_2(n+p_{12nc})...u_2(n-p_{12c}+1)]$, $\alpha = \frac{1}{1-w_{12}(0)w_{21}(0)}$ and μ is the learning gain.

Learning strategy: We assume to dispose of N samples of the mixed signals (x_1, x_2). Analysis of equations (3),(4) and (11) shows that future samples of $\mathbf{u}(n)$ - that are not available - have to be used. To circumvent this drawback we use a learning strategy consisting of initializing $\mathbf{u}(n)$ by $\mathbf{x}(n)$. Then, the learning algorithm is iterated on the data block with the updated $\mathbf{u}(n)$ until the criterion $C = \sum_{m=-max(p_{12c},p_{21nc})}^{-max(p_{21c},p_{12nc})} |R_{y_1,y_2}(m)|$ is minimized, where R_{y_1,y_2} is the cross-correlation function between y_1 and y_2.

3.2 Tests on synthetic signals

We illustrate the performance of the non-causal BSS using the two source signals $s_1(t) = \sqrt{2}sin(2\pi 0.04t) + 0.01\varepsilon_1(t)$ and $s_2(t) = \varepsilon_2(t)$, where $\varepsilon_i(t)$ are uniform white noises with unit variance. Consequently, in order to optimally match the pdf of the source signals, we choose for f_1 a hyperbolic sine function and for f_2 a piecewise linear function. The performance of our algorithm depends on the coupling factor K between channels given by equation (5). It can be characterized by the mean-squared error between the reconstructed signals and the corresponding source signals

$$MSE_i = \frac{1}{N}\sum_{n=1}^{N}\{v_i(n) - s_i(n)\}^2 \quad \text{for} \quad i = 1, 2 \qquad (12)$$

In order to detect spurious solutions we have performed simulations for various coupling factors and random parameters of the non-causal coupling filters. Results shown in figure 2 indicate that for low coupling factors ($K < 0.7$) the reconstruction of the source signal is almost perfect while for high coupling factors ($K > 0.7$) the MSE increases and spurious solutions may appear. This could be a direct consequence of the stability condition of the global system given by $K < 1$.

4 Application to the CVS

In this section we describe the interactions in the cardiovascular system and deduce from the presented model a system to blindly reconstruct $CSNA$. Finally results on clinical data are presented.

HR and ABP display spontaneous fluctuations that mainly represent interactions between the cardiac pacemaker cells and the autonomic nervous system (ANS). The ANS consists of two components, namely the *sympathetic* and the *parasympathetic* system. The sympathetic outflow increases the HR and influences ABP by constricting blood vessels. In contrast, the parasympathetic outflow reduces HR. Sympathetic and parasympathetic outflow are influenced in the baroreflex by afferent information about ABP from the baroreceptor. Representing these causal relationships leads to the bloc diagram of figure 1. Assuming that linear modeling is appropriated we can represent this loop using the linear system of figure 3a. This model includes both causal(c) and non-causal (nc) relationships.
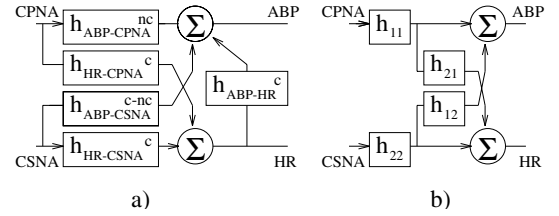

Figure 3 — Baroreceptor loop: a) non-causal model b) transformed model adapted to BSS

The model of figure 3a does not have an appropriate structure for BSS. Nevertheless we can transform it by linear operations into the model of figure 3b. But, even though the demixing filters h_{12} and h_{21} can now be obtained using BSS techniques, the determination of h_{11} and h_{22} is impossible because the signals $CSNA$ and $CPNA$ are colored noises. We solve this problem by using previous established results on the cardiovascular system [1, 9]. It can be shown that the transfer functions $H_{11}(z)$ and $H_{22}(z)$ depend on $H_{HR-CPNA}(z)$, $H_{ABP-HR}(z)$, $H_{ABP-CPNA}(z)$ and $H_{HR-CSNA}(z)$ which have low-pass transfer characteristics with their respective cutoff frequencies greater than 0.15 Hz. Therefore, the influence of $H_{11}(z)$ and $H_{22}(z)$ can be eliminated by applying a zero-phase bandpass filter (0.04-0.15 Hz) to all intervening signals. Finally we obtain the reconstruction of the $CSNA$ and $CPNA$ in the LF-band where the fundamental assumption of their mutual independence holds.

4.1 Results of blind reconstruction

In order to evaluate the performance of our algorithm we should have $CPNA$ and $CSNA$ at our disposal, but these are inaccessible signals in humans. However, since the muscle sympathetic nerve activity ($MSNA$) correlates with cardiac adrenergic activity under baseline conditions we use $MSNA$ as an indicator of $CSNA$ [10]. After bandpass filtering the

resulting $MSNA$ has a super-Gaussian pdf and we therefore choose a hyperbolic tangent function for f_i [4].

We have applied our method to clinical data acquired on five subjects. Results for blind reconstruction of $CSNA$ are presented in table 1. The performance index is the normalized mean-squared error between the blind reconstructed $CSNA$ and the measured $MSNA$ in the LF-band. Therefore a mean-squared error lower than 0.3 indicates a very satisfying reconstruction and we see that the presented observer of $CSNA$ yields good results for all five subjects.

Subject No	1	2	3	4	5
Normalized MSE	0.3	0.26	0.17	0.26	0.33

Table 1 — $CSNA$ reconstruction for 5 subjects

A typical reconstruction of $CSNA$ for a mean-squared error of 0.17 is shown in figure 4. By visual inspection we can confirm the very good quality of the blind reconstruction.
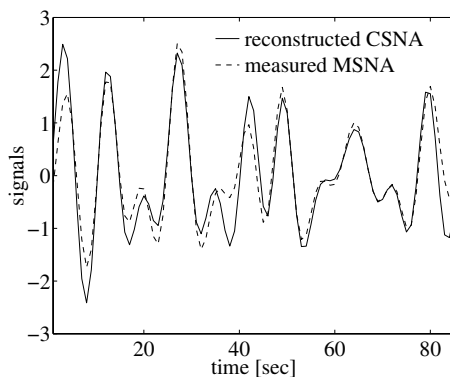

Figure 4 — Typical result for $CSNA$ observer

5 Conclusion

Applying source separation techniques we have successfully built an observer of $CSNA$ in the low frequency band (0.04-0.15Hz). The fact that blind source separation yields good results for the reconstruction of the $CSNA$ confirms the fundamental assumption we made on our clinical data about the independence of the $CSNA$ and $CPNA$. The validity of this assumption implies also that the other reconstructed signal should be the $CPNA$. This, however could not be verified because $CPNA$ is not accessible in humans.

From the clinical point of view, the presented approach is very promising because $CSNA$ and $CPNA$ could be useful for analysis and diagnosis. From the signal processing point of view, this observer constitutes an exemplary application of blind source separation techniques in biomedical engineering.

References

[1] J.P. Saul, R.D. Berger, P. Albrecht, S.P. Stein, M.H. Chen and R.J. Cohen, "Transfer function analysis of the circulation: unique insight into cardiovascular regulation", *Am. J. Physiol. Soc.*, Vol. 261, pp. H1231–1245, 1991.

[2] D.T. Kaplan and M. Talajic, "Dynamics of heart rate", *Chaos1*, pp. 251–256, 1991.

[3] M. Kollai and K. Koizumi, "Reciprocal and non-reciprocal action of the vagal and sympathetic nerves innervating the heart", *J. Autonomic Nervous System*, Vol. 1, pp. 33–52, 1979.

[4] A. Bell and T. Sejnowski, "An information-maximization approach to blind separation and blind deconvolution", *Neural Computation*, Vol. 7, pp. 1029–1059, 1995.

[5] A.B. Vallbo, K.E. Hagbarth, H.E. Torebjörk, and B.G. Wallin, "Somatosensory , proprioseptive, and sympathetic activity in human peripheral nerves", *Physiol. Rev.* , Vol. 59, pp. 919–957, 1979.

[6] C. Jutten and J. Herault, "Blind separation of sources, part 1: An adaptive algorithm based on a neuromimetic approach", *Signal Processing*, Vol. 24, pp. 1–10, 1991.

[7] K. Torkkola, "Blind separation of delayed and convolved signals with self-adaptive learning", *in ICASSP'96*, Vol. 4, pp. 229–232, 1996.

[8] A. Cichocki, S. Amari and J. Cao, "An information-maximization approach to blind separation and blind deconvolution", *in NOLTA'96*, Vol. 7, pp. 1029–1059, 1995.

[9] P. Celka, R. Vetter, U. Scherrer, and E. Pruvot, "Closed loop heart beat in terval modelization in humans using mean blood pressure, instantaneous lung volume and muscle sympathetic nerve activity", in *IEEE Annual Int. Conf. of Engineering in Medicine and Biological Society (EMBS), A msterdam*, 1996.

[10] G. Wallin, M. Esler, P. Dorward, G. Eisenhofer, C. Ferrier, R. Westerman, G. Jennings, "Simultaneous measurements of cardiac noradrenaline spillover and sympathetic outflow to skeletal muscle in humans", *J. Physiol. (London)*, Vol. 453, pp. 45–58, 1992.